

Height self-equilibration during the growth of dense nanowire ensembles: Order emerging from disorder

K. K. Sabelfeld, V. M. Kaganer, F. Limbach, P. Dogan, O. Brandt et al.

Citation: *Appl. Phys. Lett.* **103**, 133105 (2013); doi: 10.1063/1.4822110

View online: <http://dx.doi.org/10.1063/1.4822110>

View Table of Contents: <http://apl.aip.org/resource/1/APPLAB/v103/i13>

Published by the [AIP Publishing LLC](#).

Additional information on *Appl. Phys. Lett.*

Journal Homepage: <http://apl.aip.org/>

Journal Information: http://apl.aip.org/about/about_the_journal

Top downloads: http://apl.aip.org/features/most_downloaded

Information for Authors: <http://apl.aip.org/authors>

ADVERTISEMENT



Height self-equilibration during the growth of dense nanowire ensembles: Order emerging from disorder

K. K. Sabelfeld,^{1,2} V. M. Kaganer,^{1,a)} F. Limbach,¹ P. Dogan,¹ O. Brandt,¹ L. Geelhaar,¹ and H. Riechert¹

¹Paul-Drude-Institut für Festkörperelektronik, Hausvogteiplatz 5–7, 10117 Berlin, Germany

²Institute of Computational Mathematics and Mathematical Geophysics, Russian Academy of Sciences, Lavrentiev Prosp. 6, 630090 Novosibirsk, Russia

(Received 11 April 2013; accepted 8 September 2013; published online 24 September 2013)

We show that the growth kinetics of dense arrays of self-induced GaN nanowires involves the exchange of Ga atoms between nanowires: Ga atoms desorbed from the side surfaces of nanowires readsorb on neighboring nanowires. This process favors the growth of shorter nanowires and gives rise to a narrow nanowire height distribution during the late stages of growth. We propose a stochastic differential equation model which describes the growth of dense nanowire ensembles. The model calculations are in good agreement with the experiments. © 2013 AIP Publishing LLC. [<http://dx.doi.org/10.1063/1.4822110>]

The bottom-up synthesis of nanowires has provided the materials basis for exciting fundamental studies and innovative devices.¹ Towards the fabrication of nanowires with tailored properties, the microscopic growth processes,^{2–4} their effect on the resulting crystal structure,^{5–8} and the formation of more complex shapes by branching^{9–11} and kinking^{12,13} have been investigated. One key insight has been that growth processes of neighbouring nanowires interact,^{14–17} however, the consequences of this interaction have been analyzed so far only for individual nanowires. In this letter, we consider growth interactions in a large ensemble of GaN nanowires and demonstrate experimentally and theoretically a counter-intuitive collective effect of these interactions: The heights of the nanowires initially vary broadly, yet during further growth they approach a well-defined common value characterizing the macroscopic ensemble. We show that microscopically this phenomenon is mediated by the exchange of Ga atoms between neighbouring nanowires resulting from desorption and readsorption at side surfaces.

A series of GaN nanowire samples was grown on Si(111) substrates by plasma-assisted molecular beam epitaxy in the self-induced way.¹⁸ All samples were grown at the same temperature of 800 °C. The Ga and N fluxes (calibrated as growth rates of GaN films grown under N- and Ga-rich conditions, respectively¹⁹) were 4 and 18 nm/min, respectively. The growth time was the only parameter that varied from one sample to another, in the range of 15 to 120 min. The time was counted starting from the shutter opening, so that the nucleation time is included.^{20,21} The only parameter varied was the growth time.

Figures 1(a)–1(c) depict side and top view scanning electron microscopy (SEM) images of three samples, thus, representing snapshots of the ensemble evolution during growth. Figure 1(a) shows the GaN nanowire ensemble at the end of the nucleation process, and Figs. 1(b) and 1(c) follow the transformation of the ensemble in further growth. Due to the continuous rotation of the substrate during

growth, the nanowire ensemble is homogeneous over the entire wafer except for the last few millimeters at the wafer edge. The nucleation conditions were chosen such as to result in ensembles with an average distance between nanowires exceeding their diameters. The total surface coverage by nanowires varies from 30% at the end of nucleation to 43% after 120 min of growth. Consequently, the coalescence degree of these ensembles is fairly low.

The heights and diameter distributions obtained from a series of such images are presented in Figs. 1(d)–1(f). At least 200 nanowires were measured from each sample. Both the heights and diameters of individual nanowires were determined from side view SEM images similar to those presented in the left column of Fig. 1. It is evident from these data that, during growth, the initial broad height distribution splits into two parts, a narrow distribution of long nanowires and a broad distribution of short ones.

The Ga flux of 4 nm/min would result, after 120 min of growth, in a 480 nm thick planar layer. The nanowires grew more than two times longer in that time, as it is evident from Figs. 1(c) and 1(f). The faster growth of nanowires, in comparison to an equivalent planar layer, is due to the atoms impinging on their side facets and reaching their top facets by surface diffusion.^{22–24} As the material deposited on the side surface is distributed over the top facet, thinner nanowires grow faster.^{22–26} In addition to that, in a dense nanowire array, longer nanowires shadow the shorter neighbours and hence inhibit their growth. The initial ensemble of self-induced GaN nanowires already possesses a large spread in nanowire heights and diameters due to fluctuations in the nucleation process.^{20,21} The two effects described above should cause the height distribution to broaden during further growth, with thinner and longer nanowires growing faster. However, the experiment reveals the opposite behavior, as seen in Figs. 1(a)–1(c). In fact, the height distribution of the long nanowires clearly narrows.

Another type of nanowire height equilibration has been observed in vapor–liquid–solid growth,²⁷ where the Gibbs–Thomson effect in the liquid droplet on the nanowire top

^{a)}Electronic mail: kaganer@pdi-berlin.de

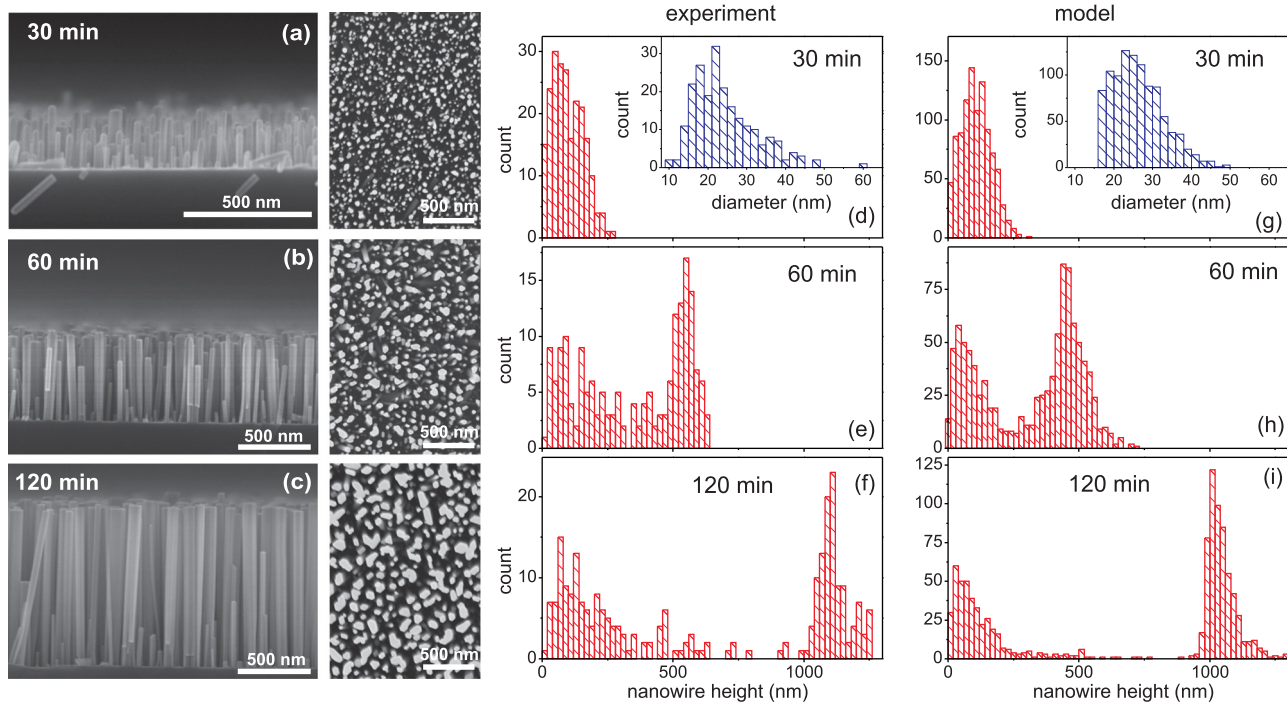


FIG. 1. (a)–(c) Side and top view SEM images of the nanowire ensemble at different stages of growth, (d)–(f) experimental nanowire height distributions obtained from the SEM images, (g)–(i) nanowire height distributions calculated by Eq. (1). The insets in (d) and (g) present the nanowire diameter distributions at the end of the nucleation process obtained from the experiment and used in the model calculations, respectively.

slows down the growth of very thin nanowires. This transient effect disappears during further growth. In contrast, the narrow height distribution observed here is self-preserving in time, as is evident from Figs. 1(b) and 1(c).

The aim of the present work is to explain this unexpected behavior. To this end, we describe the evolution of the entire nanowire ensemble by stochastic mean field differential equations. Our model includes the atomistic processes shown in Fig. 2. The source of atoms is the incoming flux from the effusion cells (labeled 1 in Fig. 2). Since the flux is inclined with respect to the substrate normal, the atoms impinge on both the top and side surfaces of the nanowires. Rotation of the substrate about its axis provides irradiation of the side surfaces from all directions. The atoms arriving at

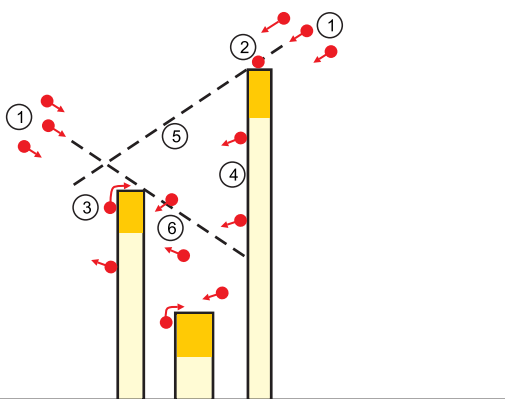


FIG. 2. A scheme of the growth of a nanowire ensemble: 1—the incoming atom flux, 2—impinging on the top facet, 3—diffusion along side surface with further contribution to growth at the top facet, 4—desorption from the side surface, 5—shadowing of short nanowires by longer neighbours, 6—adsorption of the desorbed atoms on another nanowire.

the top facet of the nanowire directly contribute to growth (process 2 in Fig. 2).

Since the N flux is large compared to both the Ga flux and the axial growth rate of the nanowires, we assume that the amount of N at the nanowire top is always sufficiently high to incorporate all available Ga atoms. This Ga-limited growth regime is the one most commonly encountered in nanowire growth.^{28–31} Under certain conditions, however, also N-limited conditions may be reached.³²

The Ga atoms impinge and diffuse on the side surface of the nanowires. The characteristic distance they migrate before desorbing is the diffusion length Λ . If the initial distance to the top surface does not exceed Λ , Ga atoms diffuse to the top surface and contribute to axial growth (process 3 in Fig. 2). The atoms impinging on the side surface at distances exceeding Λ desorb (process 4 in Fig. 2). Since the average nanowire height is larger than Λ , the atoms diffusing on the substrate do not reach the nanowire top and hence are not taken into consideration.

In contrast, N adatom diffusion along the side surface of the nanowire can be neglected as evidenced from experiments.^{32,33} This result can be understood from the fact that the N-terminated M-plane that constitute the nanowire side facets is unstable against the formation and desorption of N_2 molecules.³⁴ Thus, we follow only the impingement, surface diffusion, and desorption of Ga atoms.

For a dense nanowire ensemble, the shadowing of shorter nanowires by neighbouring longer ones also plays an important role³⁵ (line 5 in Fig. 2). However, the observed narrowing of the nanowire height distribution during growth indicates that the shorter nanowires do receive a flux in excess of the direct flux. The only possible source of material for their growth is the atoms that desorb from neighbouring

longer nanowires and readsorb on shorter nanowires (process 6 in Fig. 2). This process has been considered to contribute to the radial growth in dense nanowire ensembles.³⁶ In the present work, it is the key component needed for the nanowire height equilibration.

The processes described above can be subsumed into the following nanowire growth equation:

$$\frac{dh}{dt} = F \left[f(h) + \frac{2Z(h)\tan\vartheta}{\pi r} + \frac{\Lambda p(h)}{r^2} \right]. \quad (1)$$

Here, $h(t)$ is the nanowire height, F is the impinging flux, and the three contributions on the right hand side describe, respectively, the direct impingement on the top surface, the impingement on the side surface with subsequent diffusion to the top surface, and the readsorption (also with subsequent diffusion to the top surface) of the atoms desorbed from other nanowires. All terms in the growth equation (1) depend not only on the height of a given nanowire but also on its random surrounding, so that it is a stochastic differential equation.

To derive Eq. (1), we calculate the increase of the nanowire volume $A dh/dt$, where A is the cross-sectional area of the nanowire. Each term derived below is divided by $A = \pi r^2$, considering the nanowire as a circular cylinder of radius r . The function $f(h)$ describes the shadowing of the top facet of the nanowire by the neighboring nanowires. Let η be a random height of a neighboring nanowire. The top surface receives the direct flux as long as $h > \eta - l \cot\vartheta$, and is not irradiated otherwise. Here, l is the distance to the neighbor and ϑ is the angle between the incoming flux and the nanowire growth direction. Hence, the shadowing term is $f(h) = \theta(h - \eta + l \cot\vartheta)$, where $\theta(x)$ is the Heaviside step function, and the sticking coefficient is taken to be 1. The increase of the nanowire volume $A dh/dt$ due to the direct flux is equal to $FAf(h)$, which gives the first term in Eq. (1).

In the second term of Eq. (1), $Z(h)$ is the height of the side surface region that provides the adatom diffusion to the top facet. As long as the side surface is not shadowed by the neighbors, $Z(h)$ is equal to the diffusion length Λ on the side surface. When the neighbors partially shadow the side surface, $Z(h)$ decreases and becomes zero for a total shadowing of the side surface. A compact description of all these cases is $Z(h) = \min(\Lambda, \max(h - \eta + l \cot\vartheta, 0))$. The contribution of the side surface to the increase of the nanowire volume $A dh/dt$ is equal to $2rZ(h)F \tan\vartheta$. The product $F \tan\vartheta$ is the flux on a side facet, since F is defined as the flux on the substrate surface. The actual cross section of the nanowire exposed to the impinging flux at each time instance has a width $2r$ and the height $Z(h)$, and the nanowire rotation ensures a uniform irradiation of the nanowire from different directions.³⁷

These first two terms of Eq. (1) describe growth of nanowires directly from the incoming flux. When the distance between nanowires l exceeds the nanowire height h , shadowing does not take place and these two terms describe the growth of individual nanowires.^{22–26,38,39} The contribution of the atoms impinging on the side surface and diffusing to the top is inversely proportional to the nanowire radius r . If only these two terms are taken into consideration, the nanowire height distribution becomes broader as the nanowires grow, as we will show below.

The third term of Eq. (1) describes a collective contribution of the nanowire ensemble to the growth and is necessary to obtain a narrow nanowire height distribution. The atoms desorbed from one nanowire can readsorb on another one (process 6 in Fig. 2). Atoms desorb from a nanowire at a height level z if, first, the nanowire is not shadowed by the neighbors at this level and, second, its top absorbing part of length Λ is above this level. We take the density of desorbed atoms at a height z proportional to the total perimeter $p(z)$ of all such nanowires assuming that the distance between the nanowires is small enough and the atoms readsorb at about the same height as they desorb. Thus, $p(z)$ is calculated as the sum of perimeters of all nanowires that satisfy two inequalities, $\eta - l \cot\vartheta < z < h - \Lambda$. The total perimeter is normalized to the total number of nanowires. The contribution of the reabsorbed atoms to the increase of the nanowire volume is therefore proportional to $F\Lambda p(h)$.

Equation (1) involves not only a single nanowire but also its neighbours, so that it has to be solved for the whole nanowire ensemble simultaneously. Since the nucleation process is not considered in the present model, we take as the initial condition the nanowire distribution that is observed 30 min after beginning of deposition. With the aim to have a better statistics we use, instead of the experimental height and diameter distribution for 200 nanowires in Fig. 1(d), a similar randomly generated distribution of 1000 nanowires, as shown in Fig. 1(g). Starting with different initial distributions (including the experimental one), we find that their details are not important and further growth gives rise to the same universal distribution at later times.

Equation (1) is integrated for the whole nanowire ensemble with a constant time step of 0.1 min. After each time step, the perimeter $p(h)$ contributing to desorption for each nanowire and the average height of the long nanowires $\bar{h}(t)$ are recalculated, by counting all nanowires in the ensemble. Since the nanowire distribution becomes bimodal during growth, we calculate \bar{h} by a two step procedure as follows. First, the average height of all nanowires is obtained. Then, the average height of nanowires exceeding this value is calculated, so that only the longer nanowires are taken into account. The value \bar{h} thus obtained is close to the peak value in the nanowire height distribution. The random height of the neighbouring nanowires is taken independently for each nanowire as $\eta = (1 + 0.25\xi)\bar{h}$, where ξ is a standard Gaussian random variable with zero mean and unit variance.

Figures 1(g)–1(i) present calculations of the nanowire growth by Eq. (1). The incoming Ga flux is taken the same as in the experiment, $F = 4$ nm/min, at an angle $\vartheta = 30^\circ$ to the substrate normal, and the diffusion length is $\Lambda = 80$ nm. Our model takes into account the increase of the nanowire diameter and the distance between nanowires. This is done on average, by using the time dependencies of the average distances between nanowires $l(t)$ and the average nanowire radii $r(t)$ from the experimental plots in Fig. 3(a). The average distances between nanowires were obtained by determining the nanowire density from top view SEM images, while the average radii were obtained from the nanowire diameter distributions measured from side view SEM images together with the height distributions. The increase of the distance between nanowires and their diameters during growth is

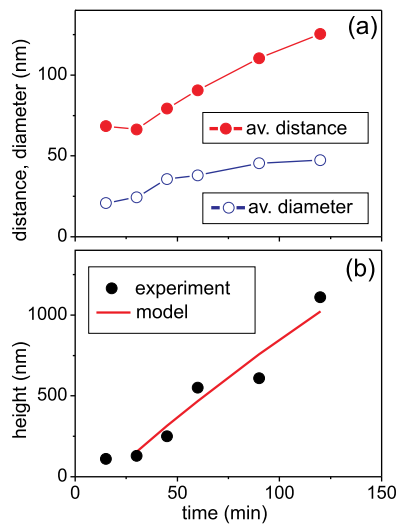


FIG. 3. Experimental time dependencies of (a) the average distance between nanowires and the average nanowire diameter and (b) measured and calculated time dependencies of the average nanowire height.

partially due to nanowire coalescence.^{40,41} Our model does not include coalescence explicitly.

The calculated nanowire height distributions reproduce very well the development of the bimodal distribution and the narrowing of the distribution of long nanowires found in the experiments. The calculated average nanowire height $\bar{h}(t)$ increases almost linearly with time, as seen in Fig. 3(b), in good agreement with the experiment. The scattering of the experimental points on the plot is due to slight fluctuations in the growth parameters from sample to sample in the series. Figure 3(b) also shows that the nucleation process ends about 30 min after the beginning of growth, thus, justifying the choice of the initial conditions in the calculations. The calculations enable us to demonstrate that the narrow nanowire height distribution in Figs. 1(h) and 1(i) is obtained due to the third term in Eq. (1) describing the growth of shorter nanowires fed by atoms desorbed from longer neighbours. When this term is excluded, a very broad height distribution is obtained in the calculations as shown in Fig. 4. If in addition shadowing is excluded by taking the distance between nanowires large enough, the height distribution does not

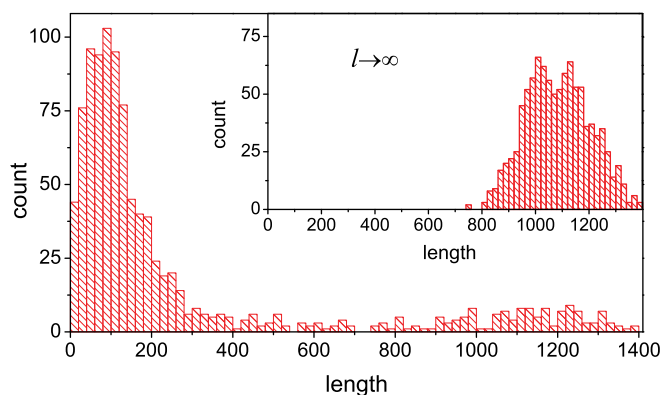


FIG. 4. Nanowire height distribution calculated by neglecting the atom exchange between nanowires. The inset shows a nanowire height distribution obtained by additionally neglecting the shadowing of nanowires (distance between nanowires $l \rightarrow \infty$). Growth time of 120 min.

contain any short nanowires (see inset in Fig. 4) and is still much broader than the experimental distribution.

Without taking into account the collective effect found here, the evolution of an entire nanowire ensemble cannot be predicted. Our model can thus be considered as a crucial step towards advanced control over the growth of nanowire ensembles. Perspectively, the methodology elaborated in this work provides the essentials for an extension towards designing the growth of arrays of differently shaped nanostructures, both in statistical or locally predefined patterns.

The work has been supported by Deutsche Forschungsgemeinschaft (DFG) Grant No. KA 3262/2-1 and Russian Fund for Basic Research Grant No. 12-01-00635.

- ¹P. Yang, R. Yan, and M. Fardy, *Nano Lett.* **10**, 1529 (2010).
- ²F. M. Ross, *Rep. Prog. Phys.* **73**, 114501 (2010).
- ³S. Hofmann, R. Sharma, C. T. Wirth, F. Cervantes-Sodi, C. Ducati, T. Kasama, and R. E. Dunin-Borkowski, *Nature Mater.* **7**, 372 (2008).
- ⁴S. H. Oh, M. F. Chisholm, Y. Kauffmann, W. D. Kaplan, W. Luo, M. Rühle, and C. Scheu, *Science* **330**, 489 (2010).
- ⁵J. Johansson, L. S. Karlsson, C. P. T. Svensson, T. Mørtensson, B. A. Wacaser, K. Deppert, L. Samuelson, and W. Seifert, *Nature Mater.* **5**, 574 (2006).
- ⁶F. Glas, J.-C. Harmand, and G. Patriarche, *Phys. Rev. Lett.* **99**, 146101 (2007).
- ⁷R. E. Algra, M. A. Verheijen, M. T. Borgström, L. F. Feiner, G. Immink, W. J. P. Van Enckevort, and E. Vlieg, *Nature* **456**, 369 (2008).
- ⁸P. Caroff, K. A. Dick, J. Johansson, M. E. Messing, K. Deppert, and L. Samuelson, *Nat. Nanotechnol.* **4**, 50 (2009).
- ⁹K. A. Dick, K. Deppert, M. W. Larsson, T. Mørtensson, W. Seifert, L. R. Wallenberg, and L. Samuelson, *Nature Mater.* **3**, 380 (2004).
- ¹⁰M. J. Bierman, Y. K. A. Lau, A. V. Kvit, A. L. Schmitt, and S. Jin, *Science* **320**, 1060 (2008).
- ¹¹J. Zhu, H. Peng, A. F. Marshall, D. M. Barnett, W. D. Nix, and Y. Cui, *Nat. Nanotechnol.* **3**, 477 (2008).
- ¹²B. Tian, P. Xie, T. J. Kempa, D. C. Bell, and C. M. Lieber, *Nat. Nanotechnol.* **4**, 824 (2009).
- ¹³K. Schwarz, J. Tersoff, S. Kodambaka, Y.-C. Chou, and F. Ross, *Phys. Rev. Lett.* **107**, 265502 (2011).
- ¹⁴L. E. Jensen, M. T. Björk, S. Jeppesen, A. I. Persson, B. J. Ohlsson, and L. Samuelson, *Nano Lett.* **4**, 1961 (2004).
- ¹⁵M. T. Borgström, G. Immink, B. Ketelaars, R. Algra, and E. P. A. M. Bakkers, *Nat. Nanotechnol.* **2**, 541 (2007).
- ¹⁶T. Gotschke, T. Schumann, F. Limbach, T. Stoica, and R. Calarco, *Appl. Phys. Lett.* **98**, 103102 (2011).
- ¹⁷A. Li, N. V. Sibirev, D. Ercolani, V. G. Dubrovskii, and L. Sorba, *Cryst. Growth Des.* **13**, 878 (2013).
- ¹⁸L. Geelhaar, C. Chèze, B. Jenichen, O. Brandt, C. Pfüller, S. Münch, R. Rothmund, S. Reitzenstein, A. Forchel, T. Kehagias *et al.*, *IEEE J. Sel. Top. Quantum Electron.* **17**, 878 (2011).
- ¹⁹B. Heying, R. Averbek, L. F. Chen, E. Haus, H. Riechert, and J. S. Speck, *J. Appl. Phys.* **88**, 1855 (2000).
- ²⁰R. Calarco, R. J. Meijers, R. K. Debnath, T. Stoica, E. Sutter, and H. Lüth, *Nano Lett.* **7**, 2248 (2007).
- ²¹V. Consonni, A. Trampert, L. Geelhaar, and H. Riechert, *Appl. Phys. Lett.* **99**, 033102 (2011).
- ²²L. Schubert, P. Werner, N. D. Zakharov, G. Gerth, F. M. Kolb, L. Long, U. Gösele, and T. Y. Tan, *Appl. Phys. Lett.* **84**, 4968 (2004).
- ²³J. Johansson, C. P. T. Svensson, T. Mårtensson, L. Samuelson, and W. Seifert, *J. Phys. Chem. B* **109**, 13567 (2005).
- ²⁴R. K. Debnath, R. Meijers, T. Richter, T. Stoica, R. Calarco, and H. Lüth, *Appl. Phys. Lett.* **90**, 123117 (2007).
- ²⁵V. Ruth and J. P. Hirth, *J. Chem. Phys.* **41**, 3139 (1964).
- ²⁶E. I. Givargizov, *J. Cryst. Growth* **31**, 20 (1975).
- ²⁷V. G. Dubrovskii, T. Xu, Y. Lambert, J.-P. Nys, B. Grandidier, D. Stiévenard, W. Chen, and P. Pareige, *Phys. Rev. Lett.* **108**, 105501 (2012).
- ²⁸M. A. Sanchez-García, E. Calleja, E. Monroy, F. J. Sanchez, F. Calle, E. Muñoz, and R. Beresford, *J. Cryst. Growth* **183**, 23 (1998).
- ²⁹S. Fernández-Garrido, J. Grandal, E. Calleja, M. A. Sánchez-García, and D. López-Romero, *J. Appl. Phys.* **106**, 126102 (2009).

- ³⁰C. Chèze, L. Geelhaar, B. Jenichen, and H. Riechert, *Appl. Phys. Lett.* **97**, 153105 (2010).
- ³¹V. Consonni, V. G. Dubrovskii, A. Trampert, L. Geelhaar, and H. Riechert, *Phys. Rev. B* **85**, 155313 (2012).
- ³²R. Songmuang, T. Ben, B. Daudin, D. González, and E. Monroy, *Nanotechnology* **21**, 295605 (2010).
- ³³R. Songmuang, O. Landré, and B. Daudin, *Appl. Phys. Lett.* **91**, 251902 (2007).
- ³⁴L. Lympirakis and J. Neugebauer, *Phys. Rev. B* **79**, 241308 (2009).
- ³⁵N. V. Sibirev, M. Tchernysheva, M. A. Timofeeva, J.-C. Harmand, G. E. Cirlin, and V. G. Dubrovskii, *J. Appl. Phys.* **111**, 104317 (2012).
- ³⁶K. A. Bertness, A. Roshko, L. M. Mansfield, T. E. Harvey, and N. A. Sanford, *J. Cryst. Growth* **310**, 3154 (2008).
- ³⁷C. T. Foxon, S. V. Novikov, J. L. Hall, R. P. Campion, D. C. I. Griffiths, and S. Khongphetsak, *J. Cryst. Growth* **311**, 3423 (2009).
- ³⁸M. C. Plante and R. R. LaPierre, *J. Cryst. Growth* **286**, 394 (2006).
- ³⁹V. G. Dubrovskii, N. V. Sibirev, R. A. Suris, G. E. Cirlin, V. M. Ustinov, M. Tchernysheva, and J. C. Harmand, *Semiconductors* **40**, 1075 (2006).
- ⁴⁰V. Consonni, M. Knelangen, U. Jahn, A. Trampert, L. Geelhaar, and H. Riechert, *Appl. Phys. Lett.* **95**, 241910 (2009).
- ⁴¹V. Consonni, M. Knelangen, A. Trampert, L. Geelhaar, and H. Riechert, *Appl. Phys. Lett.* **98**, 071913 (2011).